

NACA RM E56B02

RM E56B02

~~UNCLASSIFIED~~

Copy 160
RM E56B02



RESEARCH MEMORANDUM

REGENERATIVE-COOLING STUDIES IN A 5000-POUND-THRUST

LIQUID-OXYGEN - JP-4 ROCKET ENGINE OPERATED

AT 600-POUNDS-PER-SQUARE-INCH

COMBUSTION-CHAMBER PRESSURE

By Adelbert O. Tischler and Jack C. Humphrey

Lewis Flight Propulsion Laboratory
Cleveland, Ohio

TECHNICAL LIBRARY
AIRCRAFT MANUFACTURING CO.
9851-0051 SEPULVEDA BLVD.
LOS ANGELES 45
CALIFORNIA

CLASSIFIED DOCUMENT

This material contains information affecting the National Defense of the United States within the meaning of the espionage laws, Title 18, U.S.C., Secs. 793 and 794, the transmission or revelation of which in any manner to an unauthorized person is prohibited by law.

NATIONAL ADVISORY COMMITTEE FOR AERONAUTICS

WASHINGTON

April 17, 1956

~~UNCLASSIFIED~~

CANCELLED

Classification

CHANGED TO *Unclass*

By authority of *NACA #7* *5-29-69*

Changed by *Ked* Date *7-22-69*

NATIONAL ADVISORY COMMITTEE FOR AERONAUTICS

RESEARCH MEMORANDUM

REGENERATIVE-COOLING STUDIES IN A 5000-POUND-THRUST LIQUID-

OXYGEN - JP-4 ROCKET ENGINE OPERATED AT 600-POUNDS-

PER-SQUARE-INCH COMBUSTION-CHAMBER PRESSURE

By Adelbert O. Tischler and Jack C. Humphrey

SUMMARY


No difficulties were experienced in fuel cooling a 5000-pound-thrust liquid-oxygen - JP-4 rocket engine operated at 600-pounds-per-square-inch combustion-chamber pressure. Over-all heat-transfer rates of 1.2 Btu per second per square inch were measured at oxidant-fuel weight ratios of 2.4. The low magnitude of these heat-transfer rates may be attributed to the formation of a protective carbon insulating layer on the combustion-chamber walls. Linear extrapolation of heat-transfer rate with pressure indicates that fuel cooling at chamber pressures considerably above 600 pounds per square inch is feasible.

Specific impulses of about 90 percent of theoretical equilibrium-expansion values were obtained. At an oxidant-fuel weight ratio of 2.4 the specific impulse measured was 258 pound-seconds per pound.

INTRODUCTION

The purpose of this research was to demonstrate the feasibility of fuel cooling a liquid-oxygen - JP-4 rocket engine operating at a chamber pressure of 600 pounds per square inch and to obtain data for the heat-transfer rates at this chamber pressure.

Numerous investigations of the performance and heat-transfer rates of oxygen-hydrocarbon rocket engines have been made previously. Such measurements have been made in large-thrust fuel-cooled engines (refs. 1 and 2). The combustion-chamber pressure for these engines was of the order of 350 to 500 pounds per square inch. During the course of the investigation reported herein, data on the operation of an oxygen-gasoline engine of 28,000 pounds thrust operated at 600-pounds-per-square-inch chamber pressure were reported (ref. 3). Since JP-4 fuel and



gasoline are both hydrocarbon fuels with similar, though not identical, specific heats and heating values, the heat-transfer rates and performance figures in this report extend the data obtained previously.

The engine used for these tests was designed to produce 5000 pounds thrust. The engine characteristic length was 31.4 inches and the chamber-throat area ratio was 4. The injector was a like-on-like type with alternate rings of fuel and oxidant jet pairs.

Performance and heat-transfer data were obtained both with fuel (regenerative) cooling and with water cooling. The data are presented and briefly discussed in this report.

APPARATUS

Thrust Chamber

The thrust chamber is shown diagrammatically in figure 1. The outer and inner walls of this chamber were welded together without expansion joints to form an integral cooling-passage engine. A new fabrication technique was used as follows: An inner shell was fabricated of nickel sheet by forming, heliarc welding, and spinning over a mandrel as discussed in reference 4. Twenty-four notched ribs were heliarc welded to this inner shell. Strips of 1/32-inch Inconel sheet were formed in hand jigs (fig. 2(a)). These strips were set into the notched ribs (fig. 2(b)), and the strips and ribs were simultaneously welded together to make an integral assembly (fig. 2(c)). The welded assembly of strips formed the outer skin of the cooling jacket. This skin was reinforced with several wrappings of fiber-glass cloth (fig. 2(d)). The fiber-glass cloth was bonded by alternate layers of plastic cement.

The cooling-jacket dimensions were such that the coolant velocity at the throat of the engine was 33 feet per second at a fuel flow of 5.4 pounds per second (fuel density, 0.76 lb/cu ft). At the chamber the coolant velocity was 17 feet per second for the same flow. The pressure drop through the cooling jacket for this fuel flow was 22 pounds per square inch. The pressure drops for various fuel- and water-coolant flows are shown graphically in figure 3.

Injector

The injector used in these studies was similar to those reported in reference 1. The configuration is shown in figures 4 and 5. The injector was a like-on-like type with four fuel rings and four oxygen rings arranged alternately. There were 80 pairs of 0.055-inch oxygen holes

and 96 pairs of 0.036-inch fuel holes; 30 additional 0.031-inch fuel holes were drilled in the outer ring to spray fuel along the chamber surface.

Instrumentation

The engine was mounted on a flexure-plate thrust stand equipped with a strain-gage force-measuring cell. The flow diagram of the test rig is shown in figure 6. Chamber pressure was measured both with strain-gage transducers and with recording bourdon-tube instruments. Oxygen flow and fuel flow were each measured with two instruments, a driven-turbine flowmeter and a venturi meter equipped with differential pressure transducers. Accuracy of the individual thrust, pressure, and flow measurements was about ± 1 percent. These signals were fed into a recording oscillograph with a timing signal.

Temperatures of the coolant into and out of the engine jacket were measured with iron-constantan thermocouples with a cold-junction couple in an ice bath. No attempt was made to measure coolant temperatures at intermediate points; therefore, only over-all heat-transfer values were obtained. Liquid-oxygen temperatures were measured by copper-constantan thermocouples with the cold-junction thermocouple in a bath of liquid nitrogen. Temperatures were recorded on strip-chart recording potentiometers.

Propellants

Liquid oxygen analyzing about 0.5 percent nitrogen was obtained from a commercial vendor. This amount of nitrogen is insufficient to affect performance measurably.

The JP-4 fuel used was drawn from two batches, which varied only slightly in analysis. No additives were used in the fuel. The average analysis of the two fuel batches used is shown in table I. The variation in specific gravity and specific heat of the fuel with temperature were estimated from this analysis with the aid of correlation charts presented in reference 5. These values are represented by the following equations:

$$\text{Specific gravity} = 0.766 [1 + 5.8 \times 10^{-4} (60 - T)]$$

$$c_p = 0.458 + 0.000536 T$$

where T is in $^{\circ}\text{F}$. (Symbols used in this report are defined in appendix A.)

Pressurized helium gas was used to pump the oxidant and the fuel to the engine from 16-cubic-foot stainless-steel tanks. Flow rates were adjusted by regulating the gas supply pressure to the propellant tanks.

PROCEDURE

For the fuel-cooled runs, the JP-4 fuel supply to the engine was run first through the cooling jacket then to the injector. Coolant-flow direction was from nozzle to injector.

Two series of water-cooled runs were made, the first with water flows through the cooling jacket from 9 to 12 pounds per second, the second with flows from 6 to 7 pounds per second.

Most tests were of 10 seconds duration. One 60-second run was made with fuel cooling to show that the shorter runs gave valid heat-transfer and performance data.

The engine was started with gaseous oxygen and gaseous propane fed at relatively low pressures (20 and 16 lb/sq in., respectively) through the injector from a separate propellant supply. These propellants were ignited by a torch located at the lip of the nozzle. After burning occurred in the chamber, the main propellant supply valves were opened to obtain about 40 percent of full flow. The high-pressure liquid-propellant supply automatically closed check valves in the gaseous supply systems. After the engine operation at partial flow was deemed satisfactory, the propellant valves were opened to full flow. The full-flow running time was usually 10 seconds. At shutdown the fuel valve was closed about 0.4 second after the oxidant valve. The engine occasionally screamed very briefly during shutdown. During the course of the investigation, the rim of the injector face burned slightly. This burning shows in figure 5. Whether or not the burning was a direct result of the screaming was not ascertained.

RESULTS AND DISCUSSION

The data for the fuel-cooled runs are tabulated in table II. Specific impulse, characteristic velocity, nozzle coefficients, and over-all heat-transfer rates through the engine are plotted as functions of oxidant-fuel ratio in figure 7.

The water-cooled runs are tabulated in table III. Performance parameters are plotted in figure 8.

Theoretical performance for liquid oxygen - JP-4 fuel at 600-pounds-per-square-inch chamber pressure (ratio of chamber pressure to exit pressure, 40.8) is given by figure 9 for comparison with the experimental results.

Heat Transfer

No difficulties were encountered in operating the rocket engine with fuel cooling at 600 pounds per square inch. The temperature rise for the fuel during its passage through the cooling jacket ranged from 73° to 132° F; the over-all heat-transfer rate ranged from 1.0 to 1.4 Btu per second per square inch (fig. 7). The highest heat-transfer rates occurred at the high oxidant-fuel ratios, that is, nearest stoichiometric burning ($o/f = 3.4$). Since high o/f ratios correspond to low fuel flows as well as high combustion temperatures, operation in this mixture ratio region presents the most difficult regenerative-cooling problem.

One series of runs gave heat-transfer rates higher by about 10 percent than those for a later series. No changes were made in either the engine setup or operating procedure between these runs. These heat-transfer-rate variations may be ascribed to changes in the character or the thickness of the carbon layer formed in the engine during running.

With water cooling the heat-transfer rates were of the same magnitude as those for fuel-cooled runs (fig. 8). The rates for water flows between 9 and 12 pounds per second were slightly greater than for flows between 6 and 7 pounds per second. In this case, the slightly greater heat-transfer rates may be due in part to the colder chamber-wall surfaces with higher coolant flows. The wall-surface temperatures may also affect the carbon deposit that forms on the combustion-chamber surfaces.

Heat-transfer rates for some runs at low oxidant-fuel ratios appear out of line and higher than other corresponding values. Each of these runs was the first of a series. In order to determine whether the high heat-transfer rates occurred on the first run or at low o/f ratios a special series of four runs was made. The first and third runs were at intermediate o/f ratios; the second and fourth runs were at low o/f ratios. The results are shown in the following table:

Run	Ratio, o/f	Btu/ (sec)(sq in.), q
1	2.015	1.23
2	1.831	.96
3	2.573	1.07
4	1.709	.96

In this case the first run again gave a high heat-transfer rate when compared with the expected value. The heat-transfer rates for the remaining runs agreed with the data shown in figure 7.

The high heat transfer observed during the first run may occur because the insulating layer has not yet formed. Since no effort was made to remove the carbon deposit between runs, or between series of runs,

changes in the nature of the carbon film in the time interval between run series is indicated. The 60-second run, which was made about 2 hours after a previous series of runs, showed "normal" heat-transfer rates. Heat transfer and other performance values remained steady after 3 seconds running time whether the run was the first of a series or not. Figure 10 indicates the extent of variation of the measured parameters for the 60-second run. A slight overshoot of heat-transfer rate, never more than 105 percent of the steady-state value, was occasionally observed during the first 3 seconds running time.

Comparison with other heat-transfer results. - Most heat-transfer rates (refs. 1 and 3) in rocket engines of various sizes were obtained with fuel containing 1 percent silicone oil as an additive. The use of the silicone additive reduced the over-all heat-transfer rates by from 15 to 40 percent (ref. 1). At an oxidant-fuel ratio of 2.4 (corresponding very nearly to point of maximum theoretical specific impulse) the heat-transfer rates ranged between 0.55 and 0.65 Btu per second per square inch for combustion-chamber pressures between 300 and 500 pounds per square inch. These results were for gasoline fuel. With JP-1 fuel instead of gasoline a heat-transfer rate of 0.45 Btu per second per square inch in a 5500-pound-thrust engine was measured (ref. 1). This value was for a combustion-chamber pressure of 370 pounds per square inch at an o/f of 2.4, and the JP-1 fuel again contained silicone oil additive.

Heat-transfer rates were measured for two large engines that used JP-4 fuel without additives (ref. 2). One engine, of 75,000 pounds thrust, was operated at 385-pounds-per-square-inch combustion-chamber pressure; the other, of lightweight tubular construction and of 120,000 pounds thrust, was operated at 475-pounds-per-square-inch combustion-chamber pressure. Heat-transfer rates for the lower-thrust engine were in the neighborhood of 0.6 Btu per second per square inch. The tubular engine showed an initially high heat-transfer rate that did not appear in the data for the more massive 75,000-pound-thrust engine. The initial heat-transfer rates reached nearly 1.4 Btu per second per square inch, then fell and leveled off at about 1.1 Btu per second per square inch after approximately 3 seconds of running.

The heat-transfer values obtained at NACA at a pressure of 600 pounds per square inch were for JP-4 fuel with no additive. To compare the data of references 1 and 2 with the data of this report, corrections are needed. To correct for the effect of additives, the data of reference 1 were divided by 0.60. To correct for pressure, the data of references 1 and 2 were extrapolated linearly with pressure (see ref. 6) to 600 pounds per square inch. With these corrections, the heat-transfer data of the references agree reasonably well with the 1.1 to 1.2 Btu per second per square inch reported herein for an oxidant-fuel ratio of 2.4.

Role of carbon deposit in decreasing heat-transfer rate. - The observed heat-transfer rates are well below those calculated for a clean metal wall on the basis of classical heat-transfer equations and the thermodynamic properties of the exhaust gases. Apparently, the thin coat of carbon that was observed to form on the combustion-chamber and nozzle surfaces is an effective heat barrier.

Estimates of the over-all heat-transfer rate with various heat-transfer resistances in the surface layer were made. These rates were calculated on the basis of completely burned gas temperature throughout the chamber and are therefore somewhat high, particularly since only about 92 percent of the theoretical characteristic velocity was realized experimentally. The calculation method is given in appendix B. The results are shown graphically in figure 11.

These estimates indicate that the heat-transfer rates observed may be accounted for if the carbon surface layer has a surface temperature of about 5300° F. These calculations also indicate that without the carbon insulating layer the over-all heat-transfer rate might be of the order of 10 Btu per second per square inch.

From these results, the thickness of the carbon layer can be estimated, provided the thermal conductivity of the carbon is known. Thermal conductivities of carbon reported vary from 0.04 (lampblack) to 3.0 (petroleum coke) Btu per foot per square foot per hour per °F. If the first value listed is used, the calculated carbon-layer thickness for this engine is 0.005 inch; for a conductivity of 3.0 Btu per foot per square foot per hour per °F the thickness is 0.21 inch. No measurements of the actual carbon deposits were made, in part because of the uncertainty about what happens to the carbon layer during shutdown operations. The thicknesses of the carbon deposits after the runs appeared to be of the order of 0.01 inch.

The injector probably affects the form and thickness of the carbon layer and, in effect, the heat-rejection rate. An injector configuration (such as that used in this study) that creates conditions (presumably a fuel-rich film) for forming a thick carbon layer on the chamber surfaces will exhibit low-heat-rejection-rate characteristics. Conversely, an injector that limits the formation of a carbon layer will cause higher heat-rejection rates. The combustion chamber does not fill with carbon, because, as the carbon layer thickens, its surface temperature increases. Eventually a surface temperature (thickness) is reached where the carbon layer is "in equilibrium" with the reaction products in the combustion chamber; that is, the rate of carbon deposition is equal to the rate of carbon erosion.

Extrapolation of results to higher pressures. - The highest temperature rise in the coolant jacket during the fuel-cooled runs was 132° F

(at $o/f = 2.8$). The maximum tolerable temperature rise in the fuel without risk of film boiling or coking is unknown at present. This would depend on the local heat-transfer rates, the vapor pressure, the gum-forming characteristics of the fuel, and the coolant pressures and velocities in the chamber jacket. For a number of batches of JP-4 fuels, reference 7 reports that, at 500-pounds-per-square-inch pressure and a coolant velocity of 27.6 feet per second, a fuel temperature rise of more than 700° F is possible before film boiling occurs. At higher jacket pressures and at higher coolant velocities, still higher temperature rises in the fuel without film boiling should be possible. Here, however, a second temperature limit may occur, namely, the gum-forming or coking temperature. Presumably the thin film of coolant in immediate contact with the metal wall and therefore exposed to temperatures well above the bulk coolant temperature will form gum at these elevated temperatures. This gum then probably adheres to the metal wall. The gum coat itself, however, "cracks" to form coke. In a marginally cooled engine, any such thermal barrier between the coolant and the metal wall will result in excessive metal temperatures and wall burn-outs. Reference 7 states that coking occurred at metal-wall temperatures between 800° and 1200° F, depending apparently on the particular batch of JP-4 fuel used.

For purposes of estimating maximum chamber pressure at which a rocket engine can be regeneratively cooled with JP-4 fuel, a temperature rise of 700° F is assumed. If it is further assumed that the heat-transfer rate increases linearly with pressure (see ref. 6) and the chamber surface area is proportional to thrust, then

$$p_c \propto q = m_f (\Delta T) \bar{c}_p$$

Substituting numerical values,

$$p_{c,max} = 600 \left(\frac{700}{132} \right) \frac{0.699}{0.526} = >4000 \text{ lb/sq in.}$$

If the fuel is precooled to a low temperature, the fuel temperature rise and therefore the operating combustion-chamber pressure can be increased even further without encountering the film boiling or gum-forming temperatures. The use of a fuel with very low gum-forming tendency would also permit a higher final fuel temperature; hence, higher operating pressure.

It must be pointed out that these estimates indicate only the fuel-cooling capacity for an engine design with surface area to thrust identical with the test engine. Estimation of the local heat-transfer rates at high pressure, particularly in the nozzle throat, will depend on the detailed design (wall thickness, coolant velocities) of each particular engine, and is beyond the scope of this discussion. The low over-all

heat-transfer rates observed and the calculated cooling-capacity reserve do indicate, however, that fuel cooling at chamber pressures considerably above 600 pounds per square inch is feasible.

Performance

Experimental specific-impulse values of about 90 percent of theoretical (equilibrium expansion) were obtained at all oxidant-fuel ratios. At an oxidant-fuel weight ratio of 2.4 the specific impulse measured was 258 pound-seconds per pound. The specific impulse with fuel cooling was practically the same as with water cooling. Likewise, characteristic velocity and nozzle coefficients were comparable for the fuel- and water-cooling runs. The experimental values of nozzle thrust coefficient C_F were slightly below theoretical values. Since nozzle coefficients may be expected to be 3 to 5 percent below theoretical, these experimental values appear to be high. Careful recalibrations of the thrust, flow, and pressure-measuring equipment disclosed no persistent error, however.

These specific-impulse values agree well with data of references 1 to 3. A limited number of specific-impulse data from these sources and from this report are plotted in figure 12 against combustion-chamber pressure. Shown also is a curve for specific impulse equal to 90 percent of the maximum theoretical equilibrium specific impulse with perfect expansion to standard atmospheric pressure from each combustion-chamber pressure.

SUMMARY OF RESULTS

A 5000-pound-thrust liquid-oxygen - JP-4 rocket engine was operated at 600-pounds-per-square-inch combustion-chamber pressure with both fuel (regenerative) and water cooling. No difficulties were experienced.

Over-all heat-transfer rates of 1.2 Btu per second per square inch were measured at oxidant-fuel weight ratios of 2.4. The low magnitude of these heat-transfer rates may be attributed to the formation of a protective carbon insulating layer on the combustion-chamber walls. Linear extrapolation of heat-transfer rate with pressure indicates that fuel cooling at chamber pressures considerably higher than the 600 pounds per square inch used in these tests is feasible.

Specific impulses of about 90 percent of the theoretical values for equilibrium expansion to standard atmospheric pressure were obtained. At an oxidant-fuel weight ratio of 2.4 the specific impulse measured was 258 pound-seconds per pound.

Lewis Flight Propulsion Laboratory
National Advisory Committee for Aeronautics
Cleveland, Ohio, February 6, 1956

APPENDIX A

SYMBOLS

A	surface area, sq in.
C_F	nozzle thrust coefficient
c^*	characteristic velocity, ft/sec
c_p	specific-heat at constant pressure, Btu/(lb)(°F)
d	diameter, ft
h	heat-transfer coefficient across combustion-chamber gas boundary layer, Btu/(sec)(sq in.)(°F)
I_s	specific impulse, lb-sec/lb
k	thermal conductivity of combustion-chamber gas, Btu/(sec)(in.)(°R)
m	mass-flow rate through chamber, lb/sec
o/f	oxidant-fuel ratio
p	pressure
Q	over-all heat-transfer rate, Btu/sec
q	heat-transfer rate, Btu/(sec)(sq in.)
R	thermal resistance to heat transfer, $R = t/k$, (sq in.)(sec)(°F)/Btu
T	temperature, °F or °R
t	thickness, in.
α	half-angle of convergent section of nozzle
β	half-angle of divergent section of nozzle
μ	viscosity of gas, lb/(in.)(sec)

Subscripts:

c combustion chamber
e exit
f fuel
m metal wall, hot side
max maximum
n nozzle
t nozzle throat
s surface, hot side

Superscripts:

- average

APPENDIX B

EFFECT OF CARBON FILM ON HEAT-TRANSFER RATE

The following equations apply to the calculation of the thermal resistance of a film or layer of insulating material on the metal surface of a gas-metal-liquid heat-exchanger apparatus.

The calculations of the carbon-layer thermal resistance that would limit the heat-transfer rates to various values were based on the following steps: (1) A gas-side surface temperature for the carbon layer was assumed. (2) The heat-transfer rates for the combustion-chamber section were then calculated using the following equations:

$$q_c = h(T_c - T_s) \quad (1)$$

$$h = 0.023 \frac{k_s}{d_c} \left(\frac{4m}{\mu_s \pi d_c} \right)^{0.8} \left(\frac{T_c}{T_s} \right)^{0.8} \left(\frac{c_{p,s} \mu_s}{k_s} \right)^{1/3} \quad (2)$$

For calculating the gas-film heat-transfer coefficient h , the McAdams equation was modified so that gas properties at the carbon-surface temperature were used. In addition, properties for nonshifting (frozen) composition were used to eliminate effects due to changing gas composition. The gas properties used at various temperatures are plotted in figure 13. These correspond to an oxidant-fuel ratio of 2.43.

(3) With the heat-transfer rate thus obtained, the temperature on the hot side of the metal wall was calculated.

$$T_m = 400 + \frac{t_m q_c}{k_m}$$

The cold-side temperature was assumed to be 400° F. This assumed temperature is probably high, but, since the temperature difference across the metal-carbon layer is very high (of the order of several-thousand degrees), the error will not significantly affect the calculated results.

(4) From the difference between the hot-side (surface) and the cold-side (metal wall) carbon-layer temperatures, the resistance of the carbon layer was calculated to be

$$R = \frac{T_s - T_m}{q_c} \quad (3)$$

In order to compare the calculated heat-transfer rates in the combustion-chamber section with the over-all rates measured, it was necessary to estimate the over-all rate analytically. This was done by use of the following equations:

$$q = \frac{q_c A_c + Q_n}{A_c + A_n} \quad (4)$$

$$Q_n = \frac{0.181 k_s}{\sin \alpha} (T_c - T_s) \left(\frac{4m}{\mu_s \pi} \right)^{0.8} \left(\frac{T_c}{T_s} \right)^{0.8} \left(\frac{c_{p,s} \mu_s}{k_s} \right)^{1/3} \left[d_c^{0.2} - \left(1 + \frac{\sin \alpha}{\sin \beta} \right) d_t^{0.2} + \frac{\sin \alpha}{\sin \beta} d_e^{0.2} \right] \quad (5)$$

Simplifications inherent in these calculations are: (1) The total temperature of the combustion-chamber gases T_c was assumed to exist unchanged throughout the chamber and nozzle. (2) The assumed surface temperature of the carbon layer and the properties of the combustion-chamber gas at the surface were further assumed to be constant throughout the chamber and nozzle. (3) The nozzle was approximated geometrically by frustums of two cones joined at the nozzle throat and having half-angles α and β .

In order to avoid computational complications due to the varying heat-transfer rate and to the varying thickness of the metal wall throughout the nozzle section, the carbon-layer thermal-resistance calculations (eq. (4)) were based on the calculated heat-transfer rate and metal thickness in the combustion-chamber section only. Calculations of the carbon-layer resistance at various sections of the nozzle were not attempted. The calculated over-all heat-transfer rate (eq. (5)) was about 30 percent greater than the value for the combustion chamber (eq. (1)).

Because the calculations were intended primarily to show the qualitative effect of varying carbon-layer thickness rather than the quantitative value of this effect, radiation was neglected. Radiative heat transfer in rocket combustion chambers ordinarily amounts to about 20 percent of the convective heat transfer.

REFERENCES

1. Northup, R. P., and Weber, H. M.: Tests with Gasoline and Jet Propulsion Fuel (JP-1) in Project Hermes Rocket Motors. Rep. No. R53A0502, Guided Missiles Dept., General Electric Co., Jan. 1953. (Contract No. DA-30-115-ORD-23, Proj. Hermes TU1-2000A.)
2. Hahn, J., Gill, G., Kraus, J., and Lee, H.: Final Report on an Experimental Investigation and Study of Lox - J4 Propellant Combination in Rocket Engines in the 3000-5000 and 75,000-100,000 Lb. Thrust Ranges. Rep. No. AL-1804, North American Aviation, Inc., Nov. 11, 1953. (Contract AF33(616)-131, E.O.(R-539-17) with U.S.A.F.)
3. Hobbs, C. H.: Advanced Development of Hermes A-3B Type Propulsion Systems. Rep. No. R54A0552, Guided Missiles Dept., General Electric Co., Nov. 1954. (Contract No. DA-30-115-ORD-23, Project Hermes TU1-2000.)
4. Dalgleish, John E., and Tischler, Adelbert O.: Experimental Investigation of a Lightweight Rocket Chamber. NACA RM E52L19a, 1953.
5. Maxwell, J. B.: Data Book on Hydrocarbons. D. Van Nostrand Co., Inc., 1950.
6. Zucrow, M. J., and Beighley, C. M.: Experimental Performance of WFNA-JP-3 Rocket Motors at Different Combustion Pressures. J. Am. Roc. Soc., vol. 22, no. 6, Nov.-Dec., 1952, pp. 323-330.
7. Beighley, C. M., and Dean, L. E.: Study of Heat Transfer to JP-4 Jet Fuel. Jet Propulsion, vol. 24, no. 3, May-June 1954, pp. 180-186.

TABLE I. - JP-4 FUEL ANALYSIS

Specific gravity at 60°/60° F	0.766
Net heating value, Btu/lb	18,725
Hydrogen-carbon ratio, H/C	0.171
Aniline point, °F	138
Reid vapor pressure, lb/sq in.	2.6
Distillation at temperature, °F	
Percent evaporated:	
Initial boiling point	149
5	201
10	226
20	255
30	274
40	291
50	310
60	326
70	349
80	374
90	411
95 (final boiling point)	484
Residue, %	1.0
Loss, %	0.6

TABLE II. - SUMMARY OF DATA FOR FUEL-COOLED 5000-POUND-THRUST LIQUID-OXYGEN - JP-4 ROCKET ENGINE

Oxygen temperature, of	Oxygen mass-flow rate, lb/sec	Fuel mass-flow rate, lb/sec	Total propellant-flow rate, lb/sec	Coolant temperature, of	Coolant temperature rise, of	Over-all heat-transfer rate, Btu/(sec) (sq in.)	Chamber pressure, lb/sq in. abs	Thrust, lb	Oxidant-fuel mass ratio	Specific impulse, lb-sec/lb	Characteristic velocity, ft/sec	Nozzle thrust coefficient
-282.2	12.71	7.32	20.03	37.2	84.0	1.238	598.8	5110	1.74	255.2	5373	1.525
-284.0	12.51	6.43	18.94	37.2	83.9	1.087	557.6	4820	1.95	254.2	5280	1.543
-277.5	12.92	5.94	18.86	38.5	91.8	1.104	569.7	4880	2.17	258.4	5441	1.578
-271.8	12.92	5.61	18.53	39.6	101.4	1.162	562.4	4762	2.30	257.2	5462	1.513
-266.4	13.20	5.45	18.65	40.4	113.9	1.275	566.2	4849	2.42	259.8	5462	1.528
-289.8	12.69	6.560	19.25	59.9	73.3	.9807	589.8	4918	1.934	255.5	5518	1.489
-286.9	13.12	6.217	19.34	60.9	75.5	.8654	580.2	4986	2.110	257.9	5520	1.500
-285.0	13.20	5.174	18.37	59.7	108.3	1.171	566.7	4704	2.551	256.0	5558	1.482
-281.2	13.62	5.596	19.22	60.4	101.7	1.186	588.9	4935	2.434	256.7	5519	1.496
-280.3	13.75	5.463	19.21	60.8	106.0	1.150	588.4	4974	2.517	259.0	5517	1.510
-277.6	14.15	5.020	19.17	60.3	132.4	1.407	584.7	4901	2.819	255.4	5492	1.497
-292.7	13.75	5.454	19.20	43.8	107.2	1.201	591.8	4899	2.521	254.4	5553	1.479
-292.7	13.82	5.440	19.26	45.7	107.0	1.198	592.6	4928	2.540	255.9	5539	1.485
-292.7	13.70	5.430	19.13	46.6	103.7	1.158	587.8	4979	2.523	260.3	5533	1.512

TABLE III. - SUMMARY OF DATA FOR WATER-COOLED 5000-POUND-THRUST LIQUID-OXYGEN - JP-4 ROCKET ENGINE

Oxygen temperature, $^{\circ}\text{F}$	Oxygen mass-flow rate, lb/sec	Fuel mass-flow rate, lb/sec	Total propellant-flow rate, lb/sec	Coolant mass-flow rate, lb/sec	Coolant temperature, $^{\circ}\text{F}$	Coolant temperature rise, $^{\circ}\text{F}$	Over-all heat-transfer rate, Btu/(sec) (sq in.)	Chamber pressure, lb/sq in. abs	Thrust, lb	Oxidant-fuel mass ratio	Specific impulse, lb-sec/lb	Characteristic velocity, ft/sec	Nozzle thrust coefficient
-285.8	12.44	8.102	20.54	3.159	66.6	29.1	1.150	602.4	5132	1.535	249.9	5284	1.522
-283.2	13.34	6.545	19.88	4.273	65.1	26.8	1.097	601.6	5099	2.038	256.5	5452	1.514
-276.1	14.04	6.264	20.30	4.622	63.8	27.1	1.106	620.3	5303	2.241	261.5	5505	1.528
-274.2	15.24	5.756	21.00	4.547	51.5	33.1	1.286	638.5	5475	2.648	260.7	5477	1.531
-269.5	14.48	5.950	20.43	4.118	50.8	----	-----	627.8	5230	2.434	256.0	5534	1.524
-285.8	12.75	7.499	20.25	6.911	54.8	39.8	1.107	595.8	5036	1.700	250.1	5218	1.523
-283.1	12.70	7.274	19.97	6.387	54.0	36.6	.9501	589.7	4932	1.746	249.3	5317	1.509
-273.8	12.69	6.602	19.28	6.615	53.1	34.8	.9412	574.8	4877	1.922	254.9	5373	1.527
-273.8	13.06	6.312	19.37	6.402	52.8	36.9	.9622	589.0	4887	2.069	254.1	5480	1.492
-272.8	13.24	6.265	19.50	6.416	52.6	38.2	1.002	581.9	5006	2.113	259.0	5379	1.549
-271.8	13.66	5.738	19.40	6.416	52.4	40.7	1.068	589.3	4996	2.381	259.2	5475	1.524
-265.4	13.46	5.437	18.90	6.608	41.1	39.8	1.059	568.6	4850	2.476	259.0	5419	1.537

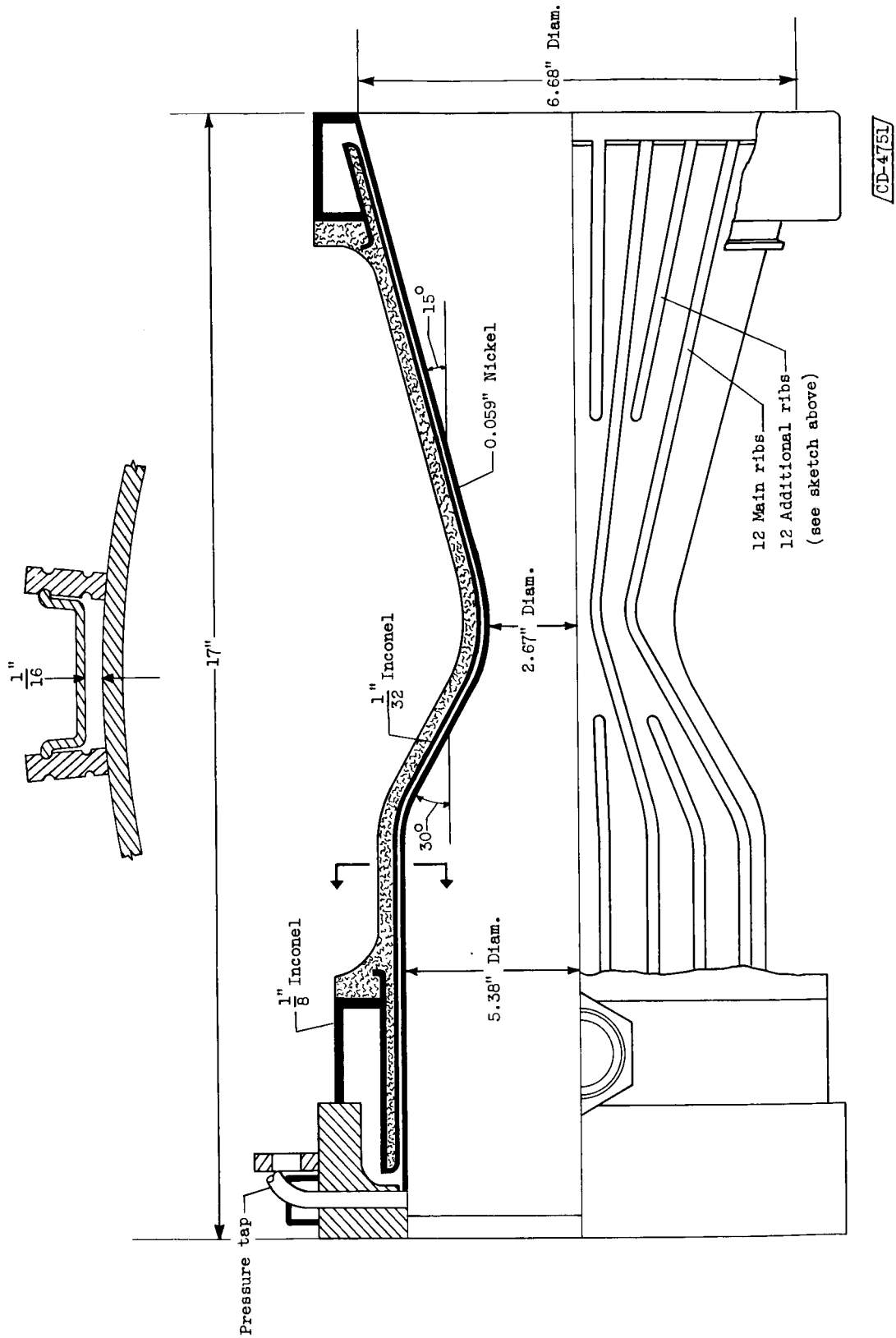
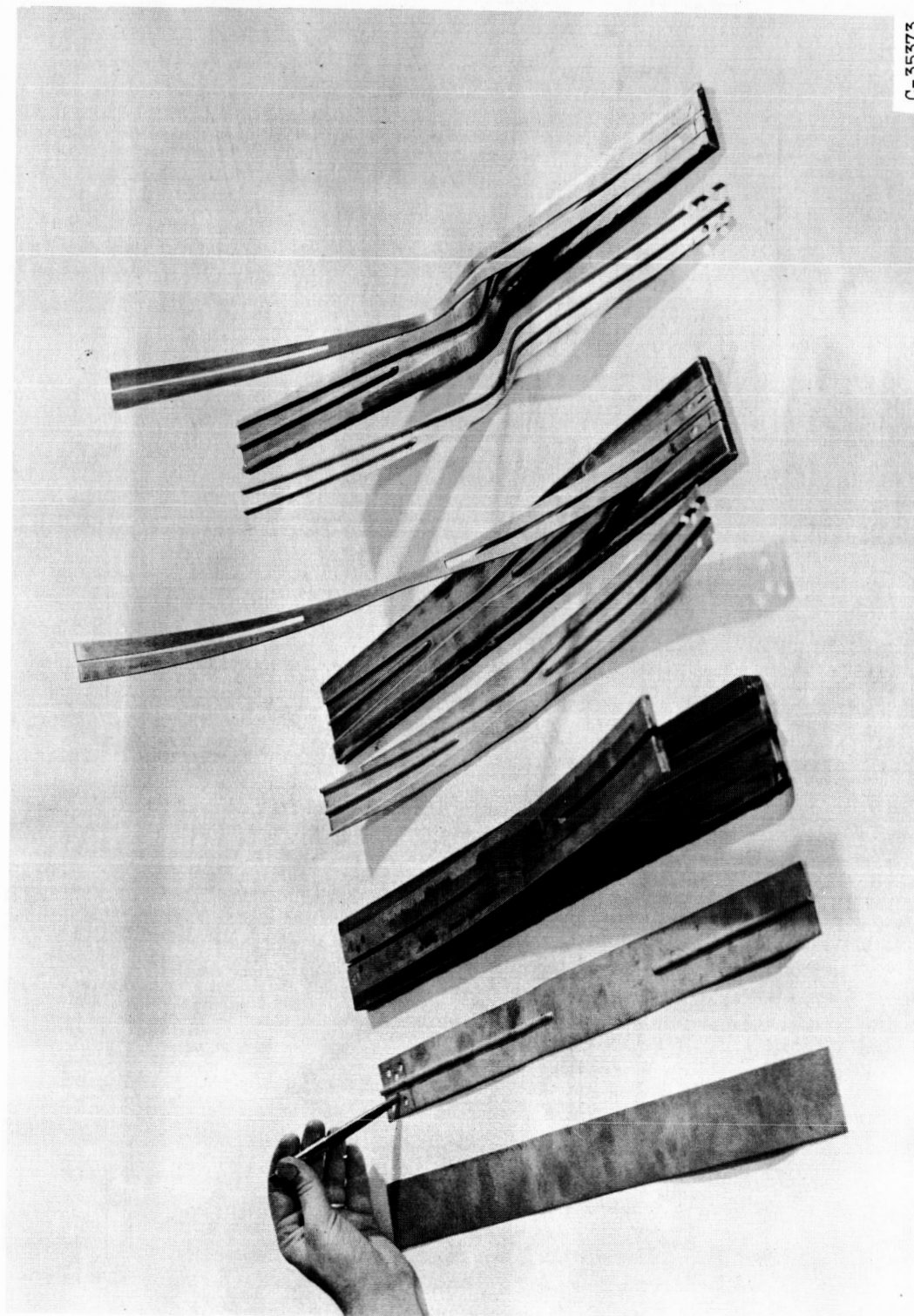


Figure 1. - Thrust chamber.



C-35373

(a) Hand jigs for making outer coolant-jacket strips.

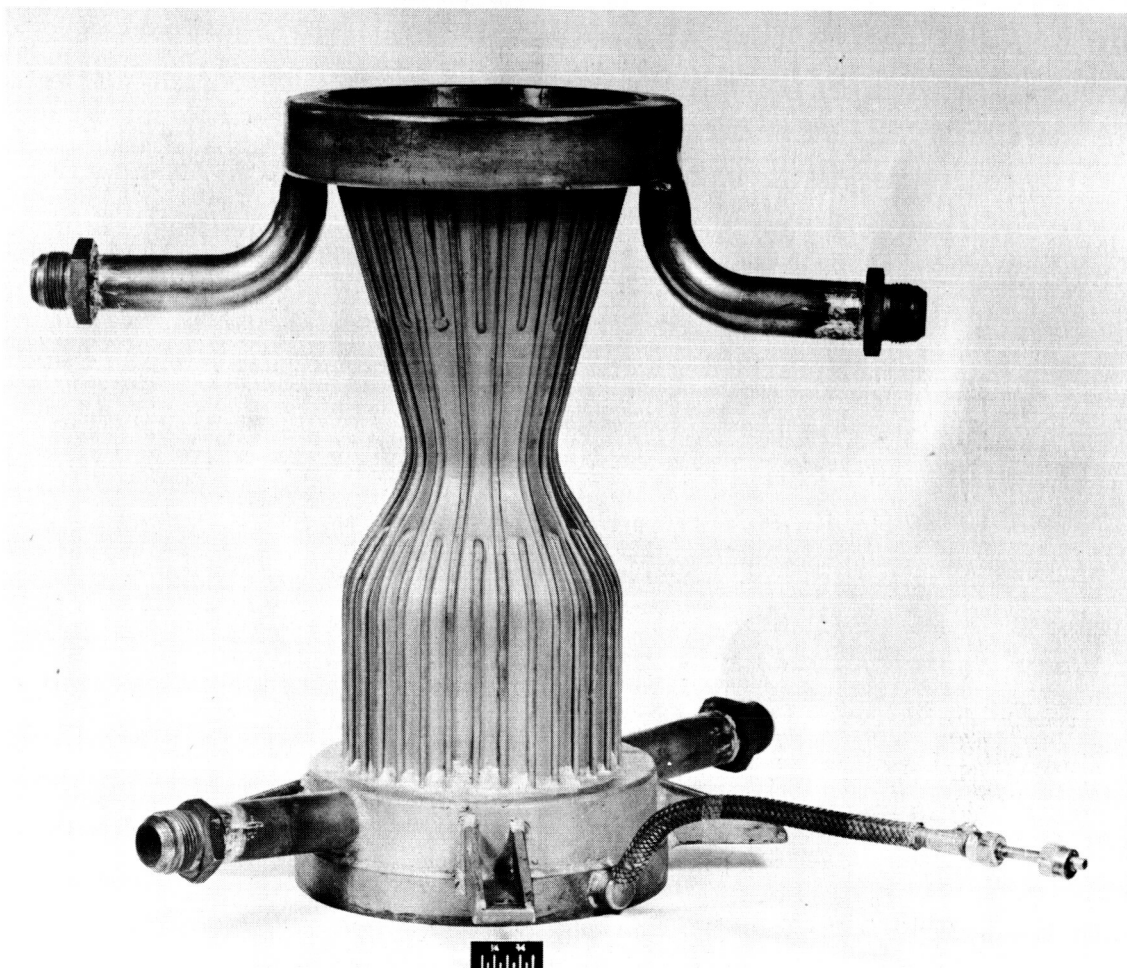
Figure 2. - Engine fabrication.



C-35374

(b) Placement of strips in notched ribs to form outer coolant-jacket wall (welding of inner ribs to inner wall incomplete).

Figure 2. - Continued. Engine fabrication.



C-37076

(c) Engine welded into integral assembly.

Figure 2. - Continued. Engine fabrication.



C-37083

(d) Final engine assembly with fiber-glass reinforcement.

Figure 2. - Concluded. Engine fabrication.

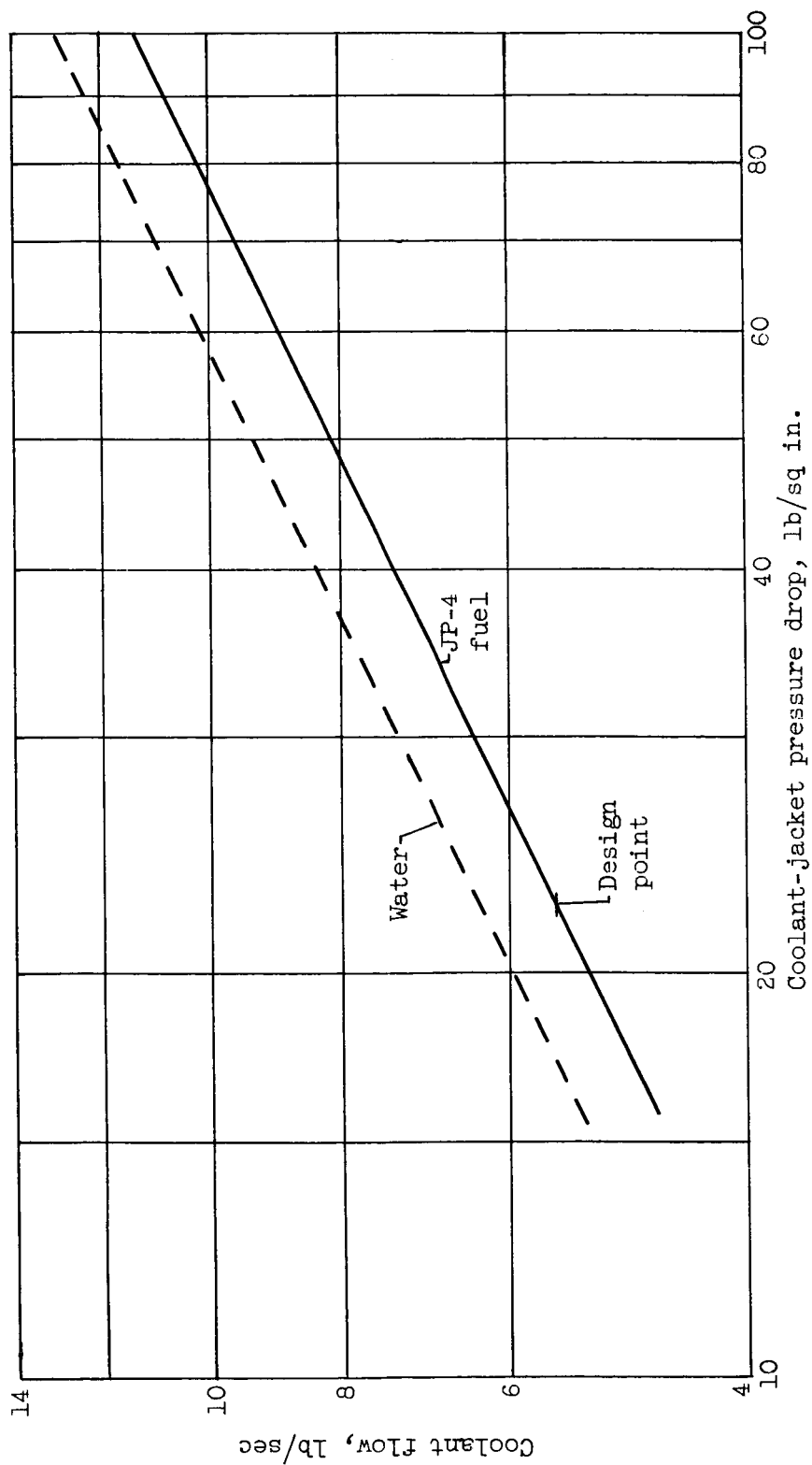
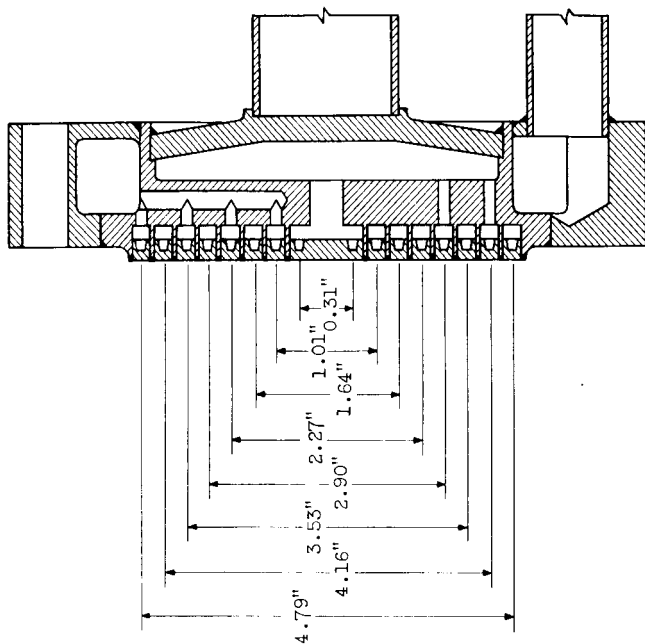
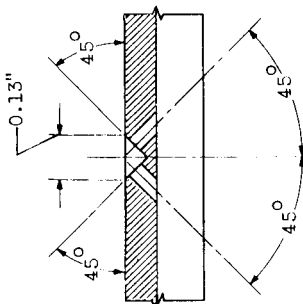
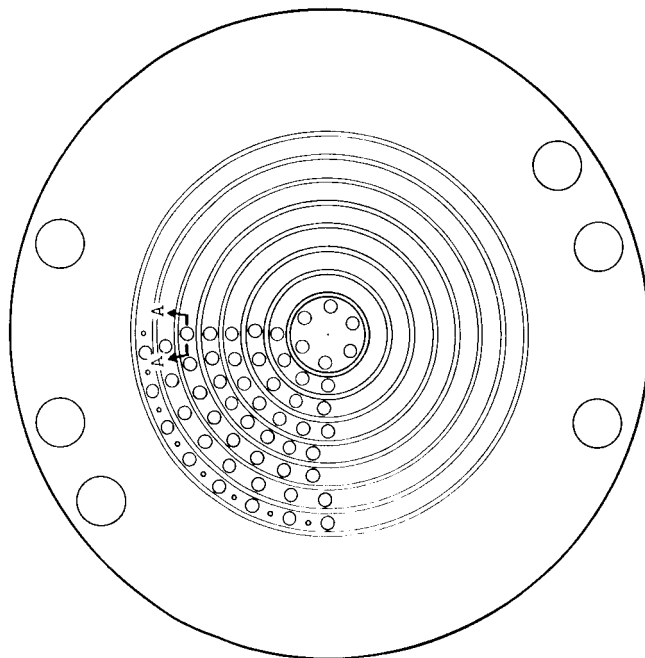


Figure 3. - Pressure drops for various fuel and water flows through engine cooling jacket.



Ring		No. of pairs of holes
Center hole	(oxidant)	6
1	(fuel)	12
2	(oxidant)	16
3	(fuel)	24
4	(oxidant)	30
5	(fuel)	30
6	(oxidant)	30
7	(fuel)	30

All oxidant holes 0.055" diam.
All fuel holes 0.036" diam.
30 Additional 0.031" holes in outer ring



Section A-A

Figure 4. - Injector.

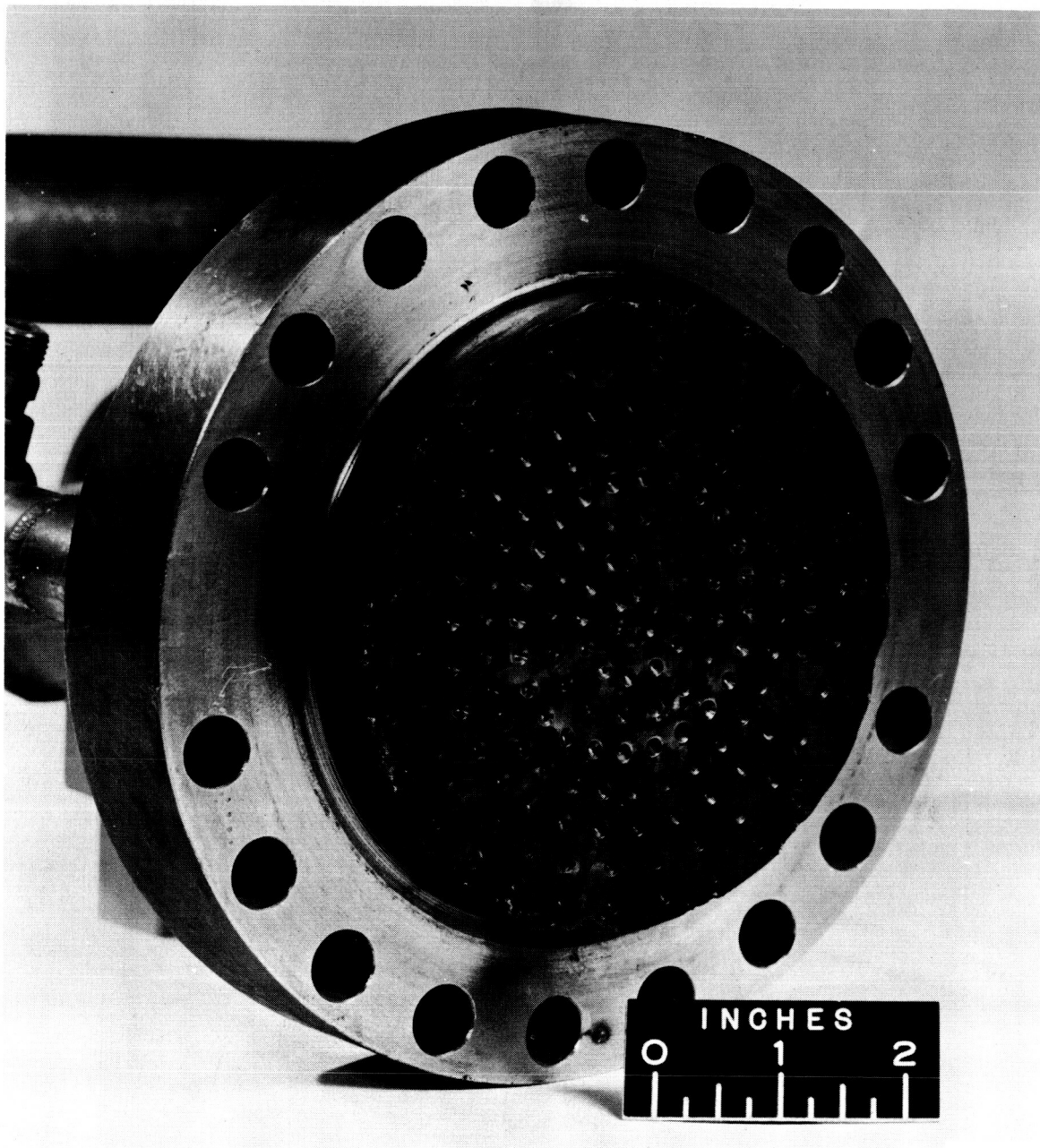


Figure 5. - Injector.

C-39373

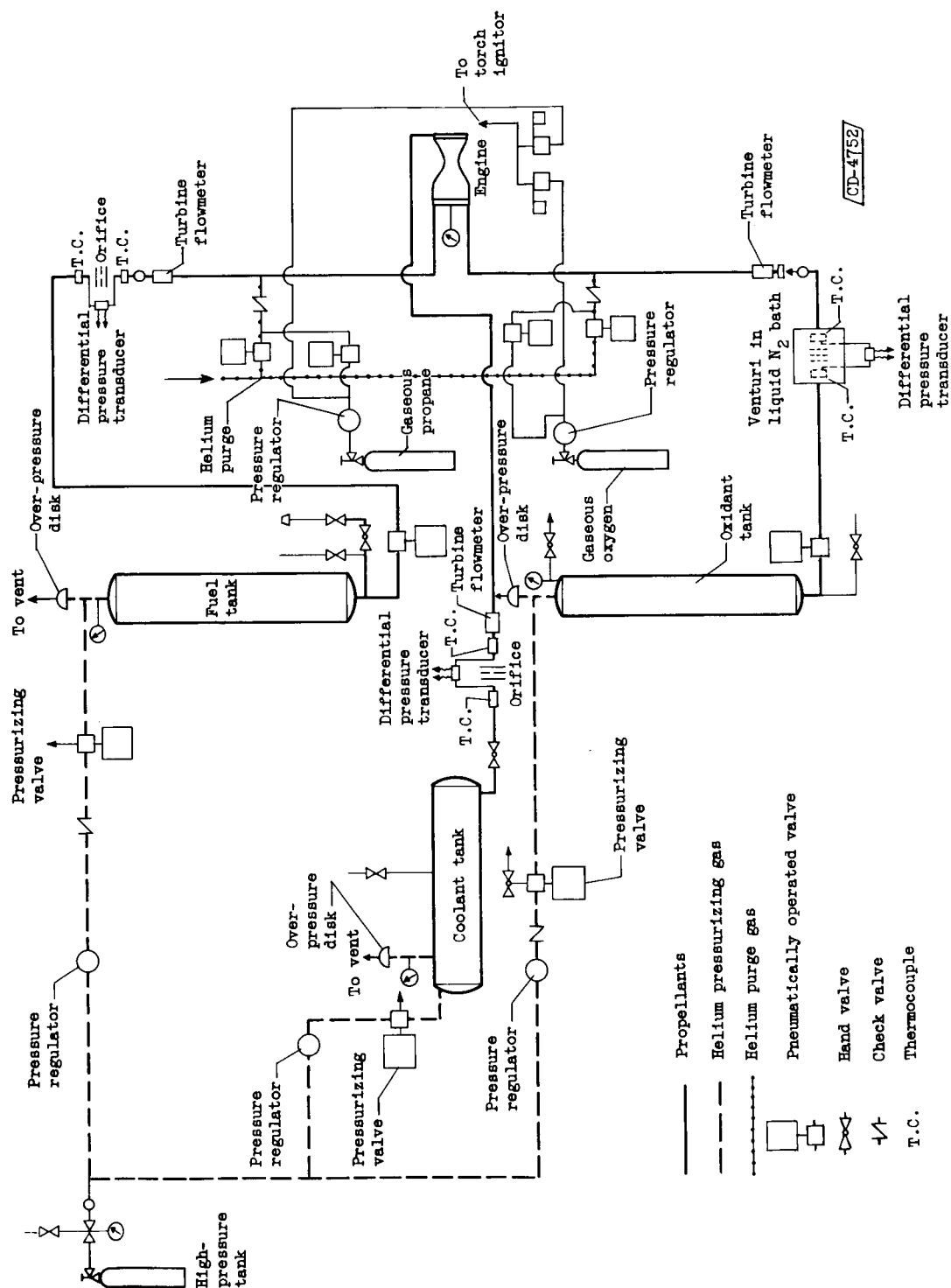


Figure 6. - Flow diagram of test rig.

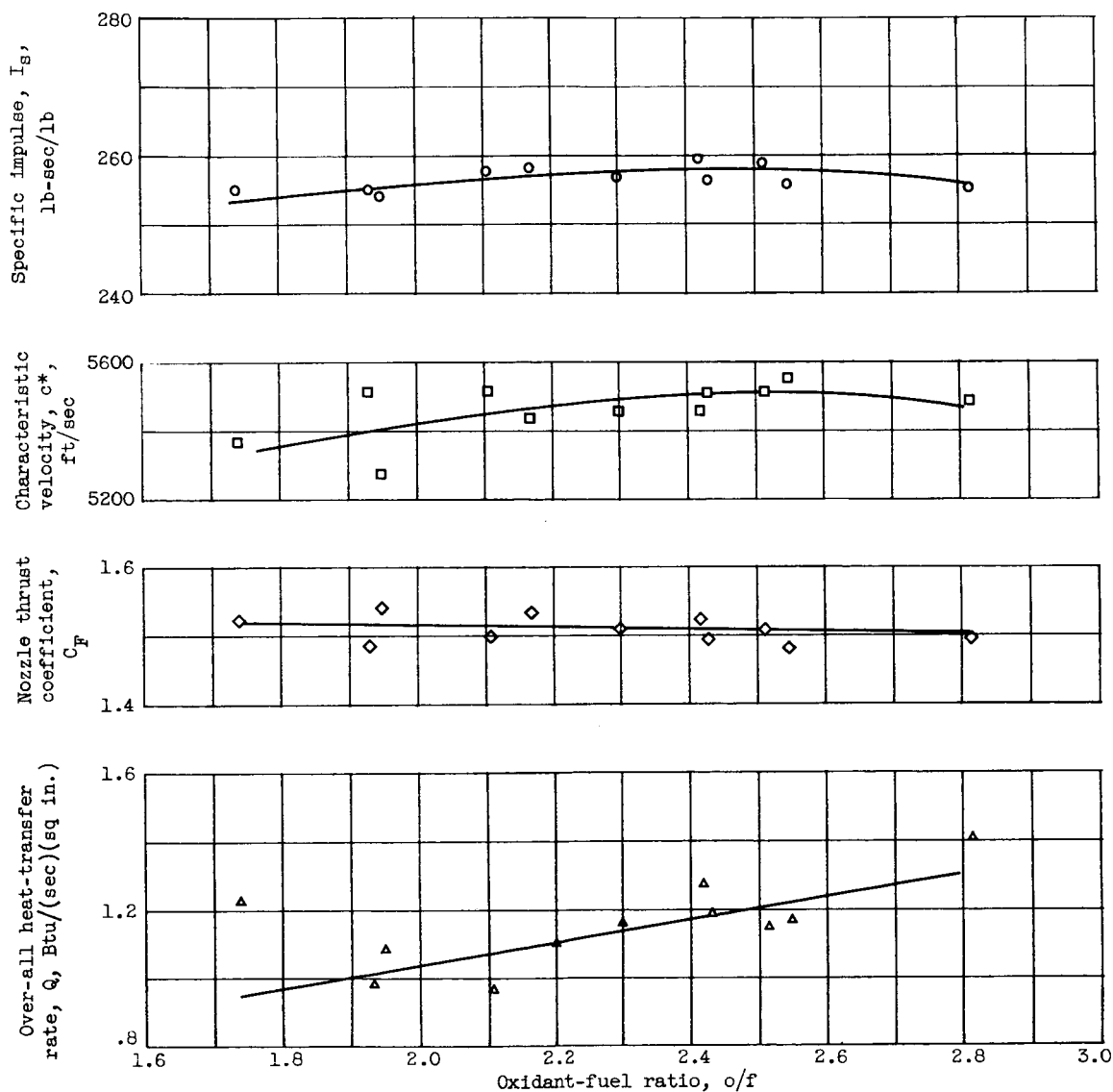


Figure 7. - Performance and heat-transfer data for fuel-cooled runs. 5000-Pound-thrust liquid-oxygen - JP-4 rocket engine.

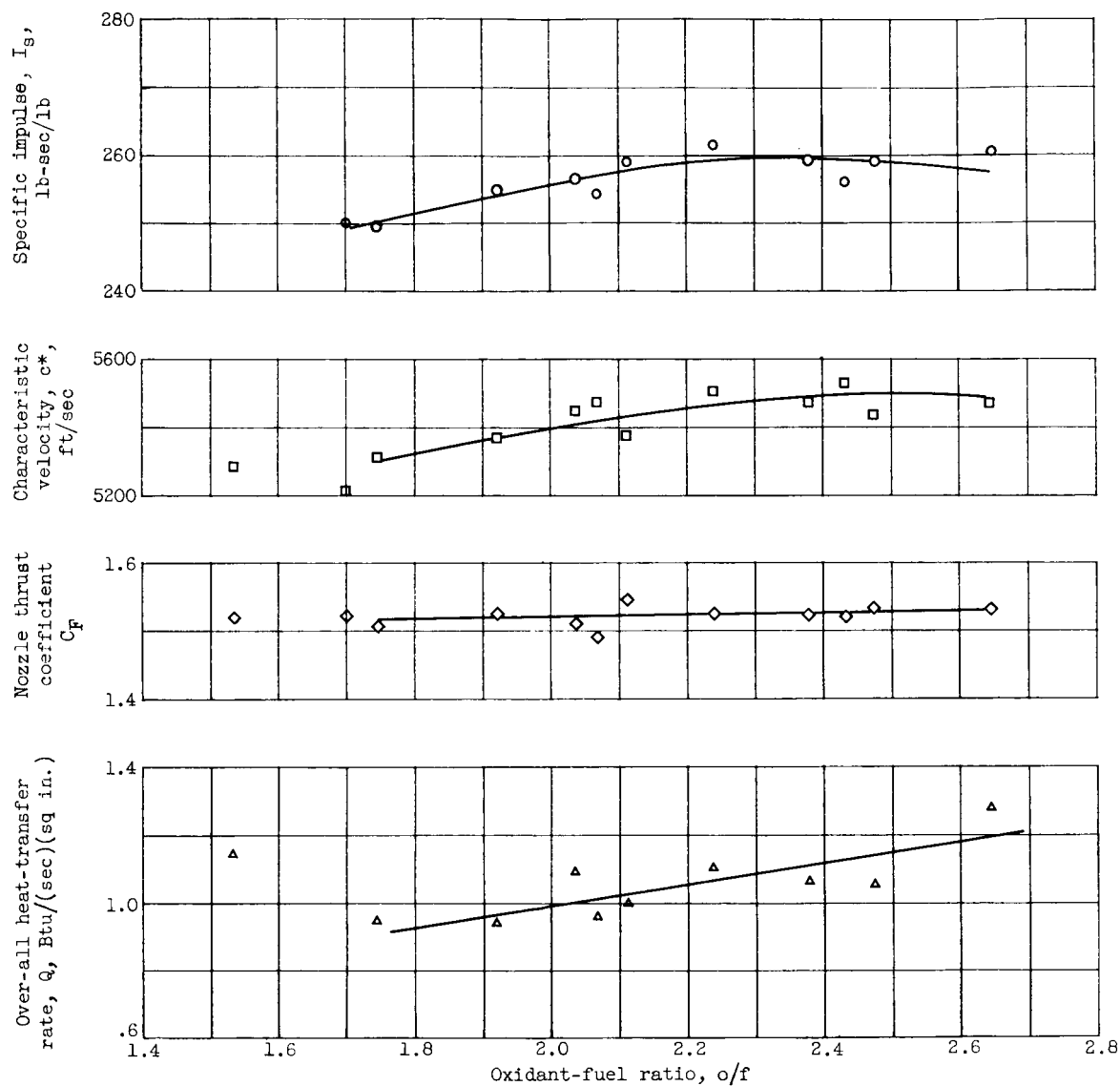


Figure 8. - Performance and heat-transfer data for water-cooled runs. 5000-Pound-thrust liquid-oxygen - JP-4 rocket engine.

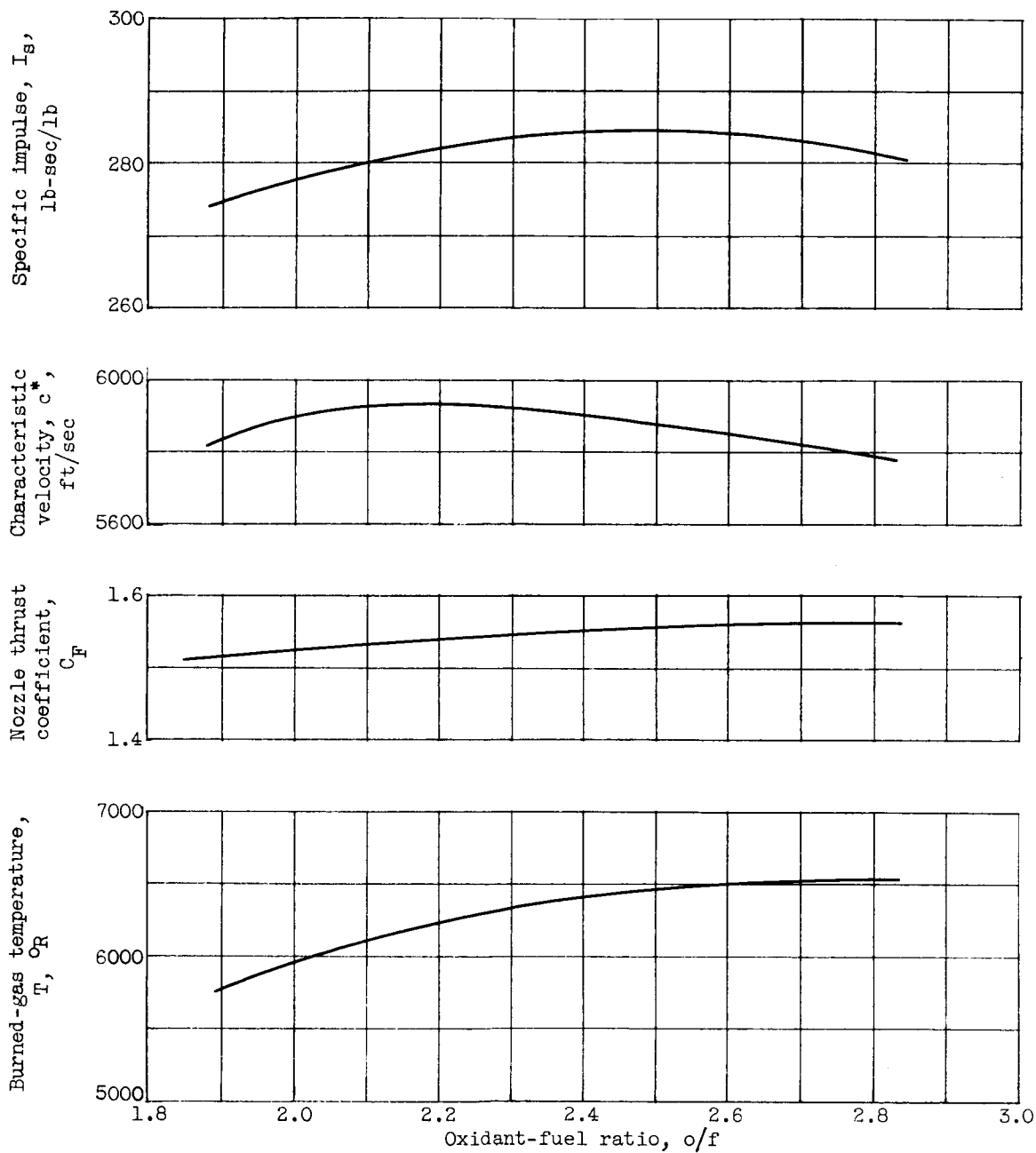


Figure 9. - Theoretical performance data for liquid oxygen and JP-4 fuel propellants at 600-pounds-per-square-inch pressure. Ratio of chamber pressure to exit pressure, 40.8.

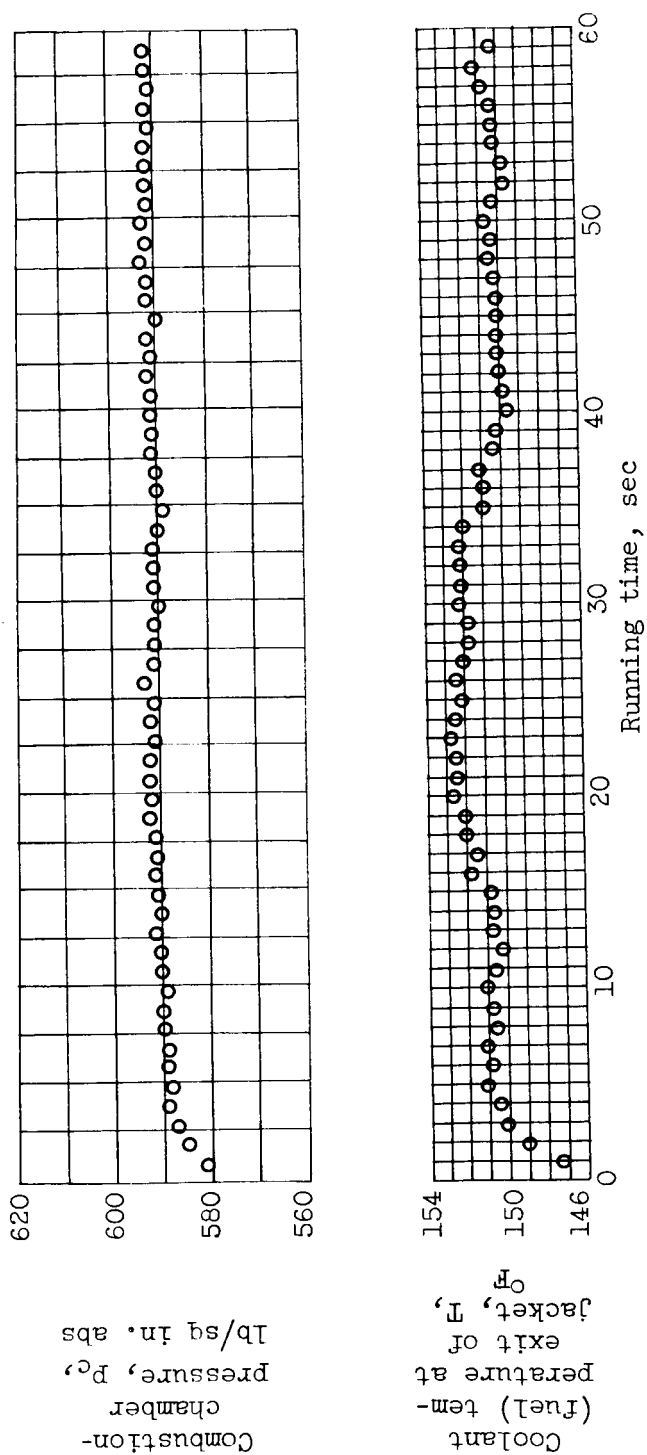


Figure 10. - Variation of combustion-chamber pressure and fuel temperature at exit of coolant jacket with length of run.

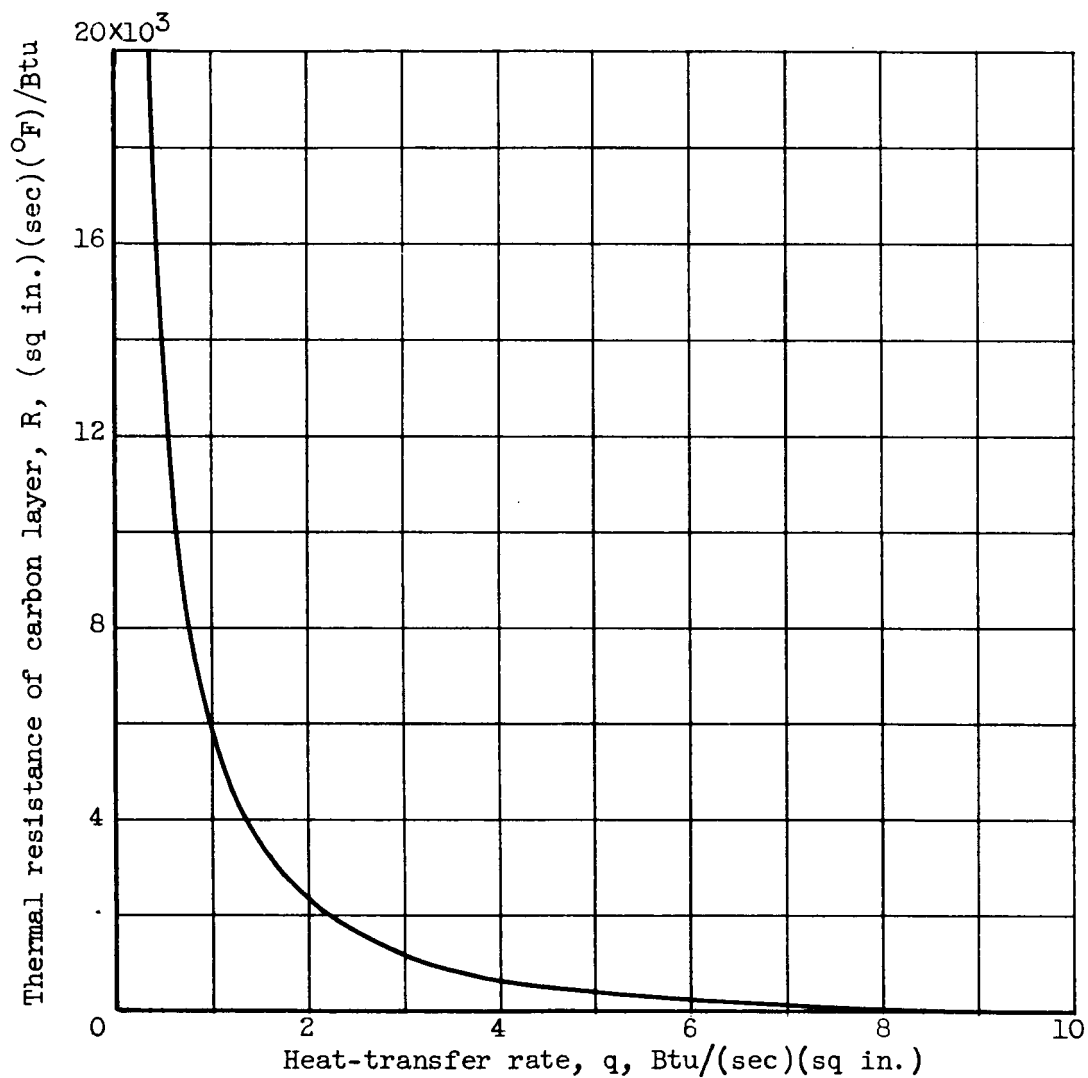


Figure 11. - Calculated relation between heat-rejection rate and thermal resistances of the carbon surface layer.

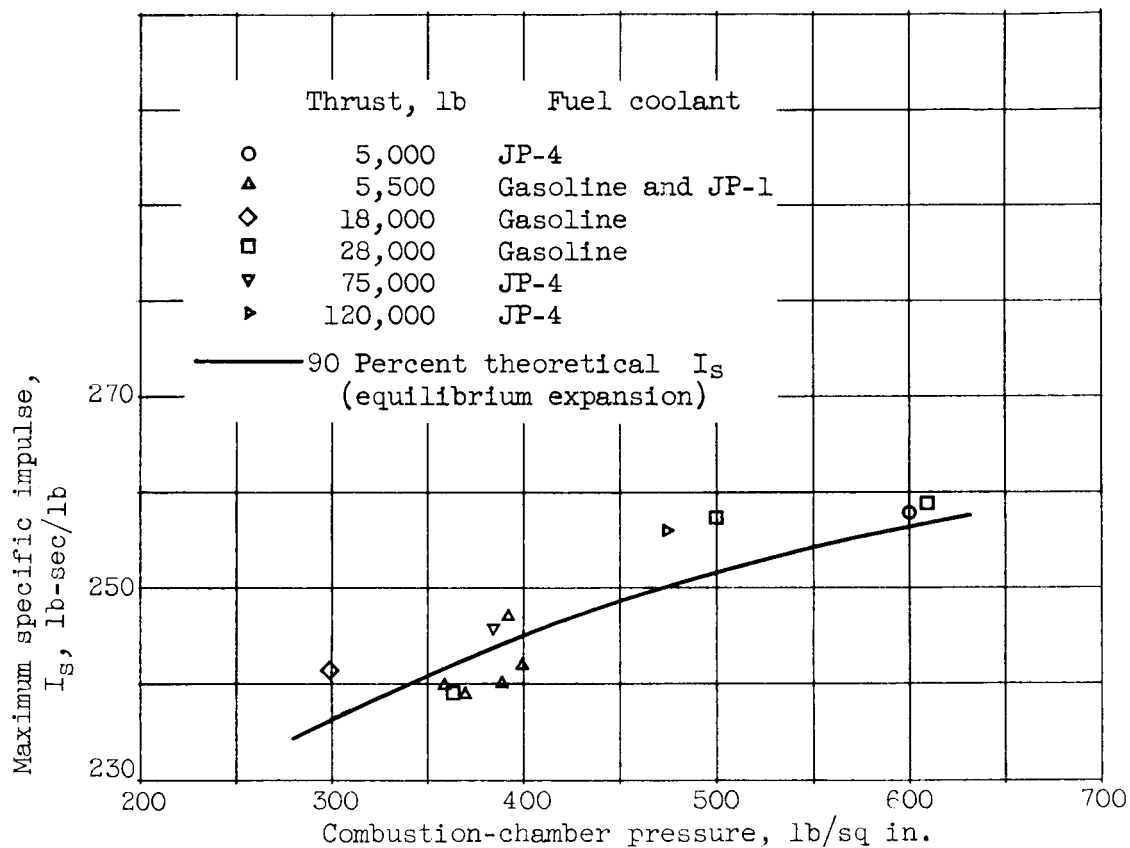


Figure 12. - Experimental specific impulse as function of combustion-chamber pressure.

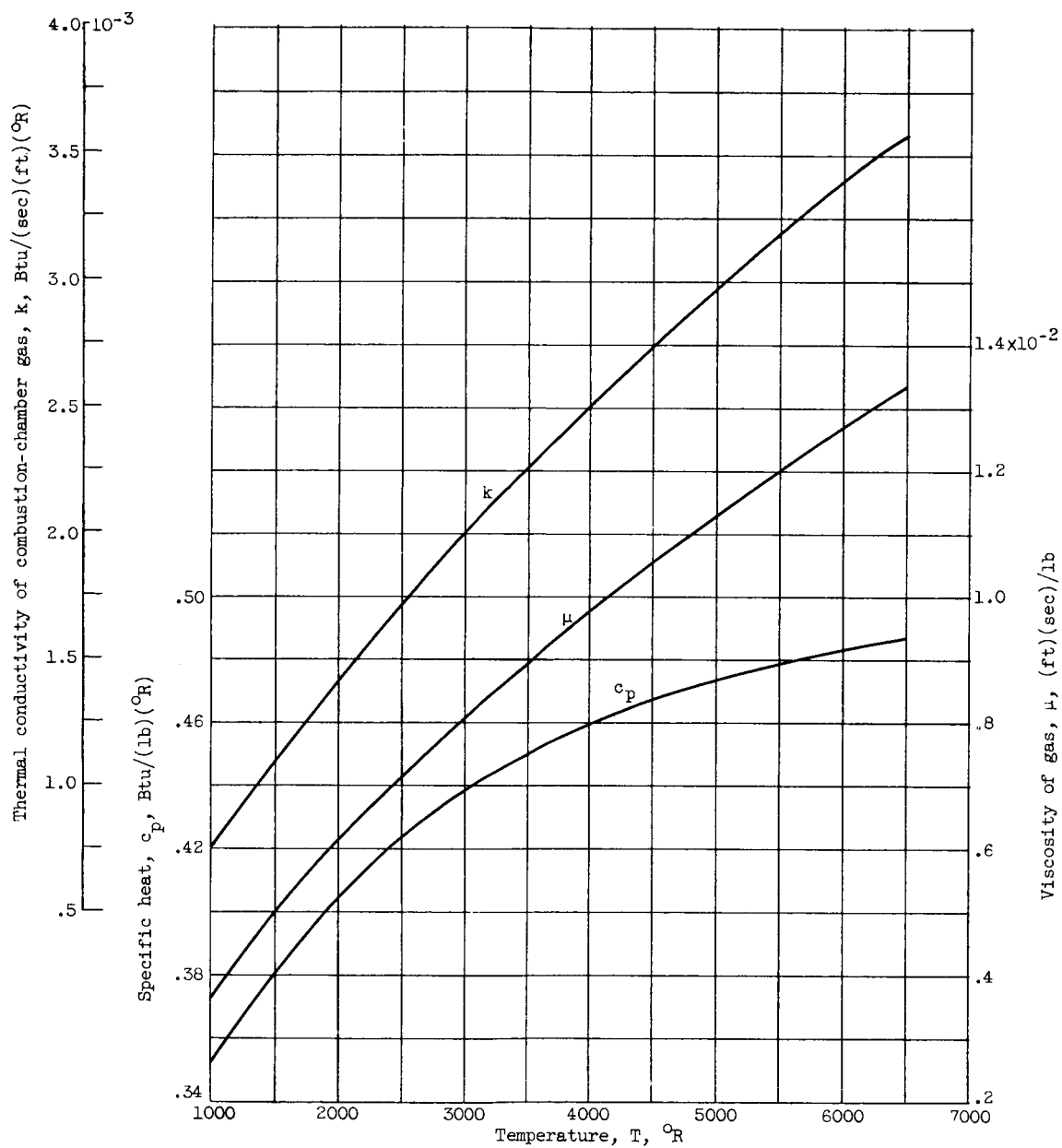


Figure 13. - Rocket exhaust-gas properties at elevated temperatures.
Frozen-composition values; oxidant-fuel ratio, 2.43.